Oncogene (2001) 20, 1981 – 1989

www.nature.com/onc

Reverse phase protein microarrays which capture disease progression show activation of pro-survival pathways at the cancer invasion front

Cloud P Paweletz[1,2,3], Lu Charboneau[2], Verena E Bichsel[1,2], Nicole L Simone[2], Tina Chen[2], John W Gillespie[4], Michael R Emmert-Buck[5], Mark J Roth[6], Emanuel F Petricoin III[1] and Lance A Liotta*[,2]

[1]Tissue Proteomics Unit, Division of Therapeutic Proteins, CBER, Food and Drug Administration, Bethesda, Maryland, MD 20892, USA; [2]Laboratory of Pathology, National Cancer Institute, National Institutes of Health, Bethesda, Maryland, MD 20892, USA; [3]Georgetown University, Department of Chemistry, Washington, District of Columbia, DC 20057, USA; [4]Cancer Genome Anatomy Project, Office of the Director, National Cancer Institute, National Institutes of Health, Bethesda, Maryland MD 20892, USA; [5]Pathogenetics Unit, Laboratory of Pathology, National Cancer Institute, National Institutes of Health, Bethesda, Maryland, MD 20892, USA; [6]Cancer Prevention Studies Branch, National Cancer Institute, National Institutes of Health, Bethesda, Maryland, MD 20892, USA

Protein arrays are described for screening of molecular markers and pathway targets in patient matched human tissue during disease progression. In contrast to previous protein arrays that immobilize the probe, our reverse phase protein array immobilizes the whole repertoire of patient proteins that represent the state of individual tissue cell populations undergoing disease transitions. A high degree of sensitivity, precision and linearity was achieved, making it possible to quantify the phosphorylated status of signal proteins in human tissue cell subpopulations. Using this novel protein microarray we have longitudinally analysed the state of pro-survival checkpoint proteins at the microscopic transition stage from patient matched histologically normal prostate epithelium to prostate intraepithelial neoplasia (PIN) and then to invasive prostate cancer. Cancer progression was associated with increased phosphorylation of Akt ($P<0.04$), suppression of apoptosis pathways ($P<0.03$), as well as decreased phosphorylation of ERK ($P<0.01$). At the transition from histologically normal epithelium to PIN we observed a statistically significant surge in phosphorylated Akt ($P<0.03$) and a concomitant suppression of downstream apoptosis pathways which proceeds the transition into invasive carcinoma. *Oncogene* (2001) **20,** 1981 – 1989.

Keywords: laser capture microdissection; protein microarrays; apoptosis; Akt; mitogen activated protein kinase; tumor progression

Introduction

The activated (e.g. phosphorylated) state of signal pathway checkpoints *in vivo* can not be ascertained from gene expression alone (Williams and Hochstrasser, 1997). Nevertheless, the state of such pathways may be a key determinant of diseased cellular physiology such as early stage cancer. In glandular tissue such as breast and prostate, malignant neoplasia originates in microscopic lesions, which evolve over time. Stationary flat epithelium and myoepithelium, is replaced by the piling up of multiple layers of neoplastic cells within the duct or gland lumen. As time proceeds, there is a transition to invasive carcinoma. The hallmark of invasion is disruption of the periglandular basement membrane, and the migration of neoplastic cells into the surrounding stroma. It is now understood that premalignant progression taking place in such microscopic lesions may be the outward manifestation of a complex tissue microenvironment, in which positive and negative interactions are taking place between organ parenchymal cells, stroma, blood vessels, and the extracellular matrix (Hanahan and Weinberg, 2000). At any point in time the summation of these interactions is reflected in the activation of signal transduction networks in the tissue cells. Cell culture systems, and even animal carcinogenesis models, may not accurately represent the complexity and the true physiologic state of the diseased human tissue (Page *et al*., 2000; Ornstein *et al*., 2000). Consequently we sought to develop a new means to analyse the state of critical signaling proteins within the individual cell types comprising the evolving premalignant lesion in human tissue.

Immunohistochemistry can provide clues to the abundance of cellular protein antigens in tissue. However, immunohistochemistry is not suitable for the analysis of subtle quantitative changes in multiple classes of proteins taking place simultaneously within an individual cell type. Such subtle changes may make all the difference in the slow progression of precancerous lesions over many years. In particular, changes in the activation status of signal pathway circuits that regulate downstream cell cycle progression and pro-survival can generate an imbalance, which ultimately results in the loss of cell growth control and the net

*Correspondence: LA Liotta
Received 22 November 2000; revised 10 January 2001; accepted 15 January 2001

accumulation of neoplastic cells. Small reductions in the apoptotic rate, which normally balances cell death against the cell population birth rate, will cause cell population growth. Growth is further stimulated if progression through the cell cycle is perpetuated rather than being checked as it might be during differentiation. We therefore set out to develop a highly quantitative and precise protein array technology that could ascertain the changing state of protein circuitry regulating growth and survival in microscopic premalignant lesions and invasive carcinoma from human tissue specimens.

Protein microarrays are now being designed to investigate large study sets of protein interactions in parallel similar to gene expression arrays recently used in functional genomics (Emili and Cagney, 2000; Fodor *et al*., 1991; Kononen *et al*., 1998; MacBeath *et al*., 1999; Ge, 2000; Englert *et al*., 1999; Lueking *et al*., 1999; Arenkov *et al*., 2000; Ekins and Chu *et al*., 1991; Rowe *et al*., 1999; Jones *et al*., 1998; Buckholtz *et al*., 1999). However, in contrast to previous antibody-, ligand-, or heterogeneous tissue fragment arrays, which mostly incorporate the use of single probes, our reverse phase protein array immobilizes whole protein lysates from histopathologically relevant cell populations procured by Laser Capture Microdissection. The array is designed to capture various stages of microscopic progressing cancer lesions within individual patients. Furthermore, each patient set is arrayed in miniature dilution curves to facilitate accurate quantification and enlarge the dynamic range. In contrast to previous antibody arrays, ligand arrays, or heterogeneous tissue fragment arrays, our protein array contains immobilized proteins from pure microdissected human tissue cells.

We have applied this microarray to analyse, in human tissue, the state of checkpoints for pro-survival and growth regulation at the transition from histologically normal epithelium, to Prostate Intraepithelial Neoplasia (PIN) and into prostate carcinoma at the invasion front.

Results

Precision, specificity and dynamic range of reverse phase protein arrays

Reverse phase protein microarrays combine laser capture microdissection (LCM) (Emmert-Buck *et al*., 1996) and cDNA microarray technologies (Schena *et al*., 1995; De Risi *et al*., 1996; Lipshutz *et al*., 1999). First, histophathological relevant cell populations are microdissected, lysed in a suitable lysing buffer, and approximately 3 nL of that lysate are arrayed with a pin based microarrayer onto glass backed nitrocellulose slides at defined positions. These applications result in 250–350 μm wide spots each containing the whole cellular repertoire corresponding to a given pathologic state that has been captured. Subsequently, each slide can be probed with an antibody that can be detected by fluorescent, colorimetric, or chemiluminescent assays (Figure 1). Over 1000 individual cellular lysates can be accommodated on a 20×30 mm slide with 1 μl of lysate.

We tested the precision and linearity of our platform using microarrayed dilution curves or recombinant prostatic specific antigen (PSA). Twenty standard curves of 20 fg to 1.25 fg were arrayed on each slide. This experiment was carried out between seven different slides providing ultimately 140 data points for analysis. Intra spot reproducibility was measured by taking the mean intensity of 20 individual applications for a given concentration within a slide and comparing it to the mean intensity of the remaining six slides. Two representative chromogen stained arrays of this experiment are shown in Figure 2a. Incubating the array with IgG isotype matched mouse control antibody and secondary antibody alone as negative controls yielded no detectable signal (data not shown). Linear correlations were observed for individual rows on each array with r^2 values ranging from 0.999 to 0.990 (Figure 2c). Analysis of inter and intra spot reproducibility and linearity showed good correlation over the examined curve with a correlation coefficient r^2 of 0.973 (Figure 2d). The detection limit (defined as two standard deviations above background) was found to be at least 10^{-21} mol for recombinant PSA, while the 'functional sensitivity' defined as the lowest concentration measured with a CV% of 20% within an array was determined to be 5×10^{-20} mol. Nevertheless, the sensitivity of individual antibody antigen interactions for any given detection system are highly dependent on the relative abundance of the antigen antibody species and the binding affinities between the probe antibodies and the immobilized antigens (Haab *et al*., 2000).

To test whether microdissected lysates can be applied on our array format, we arrayed triplicate dilution curves from LCM procured esophageal normal epithelial cell lysates ranging from 120×10^{-4} to 4×10^{-4} cell equivalencies per array spot on seven slides. Arrays were probed against annexin-1 (Figure 3a). Good linearity and reproducibility from sample to sample with r^2 of 0.952 was shown for the whole dataset analysed (Figure 3b). The coefficient of variance for inter and intra spot reproducibility ranges from 1.66 and 1.25% at high cellular concentration to 21.18 and 39.4% (intra and inter spot reproducibility, respectively) at the limit of detection (Figure 3c). Negative control slides yielded no detectable signal. These results reveal that the micro application of recombinant and microdissected protein lysates onto nitrocellulose slides can be applied reproducibly and quantifiable.

Candidate validation in human tissue

We recently reported that annexin-1 protein expression in squamous esophageal and prostate cancer is significantly less than that found in adjacent normal epithelium (Emmert-Buck *et al*., 2000; Paweletz *et al*.,

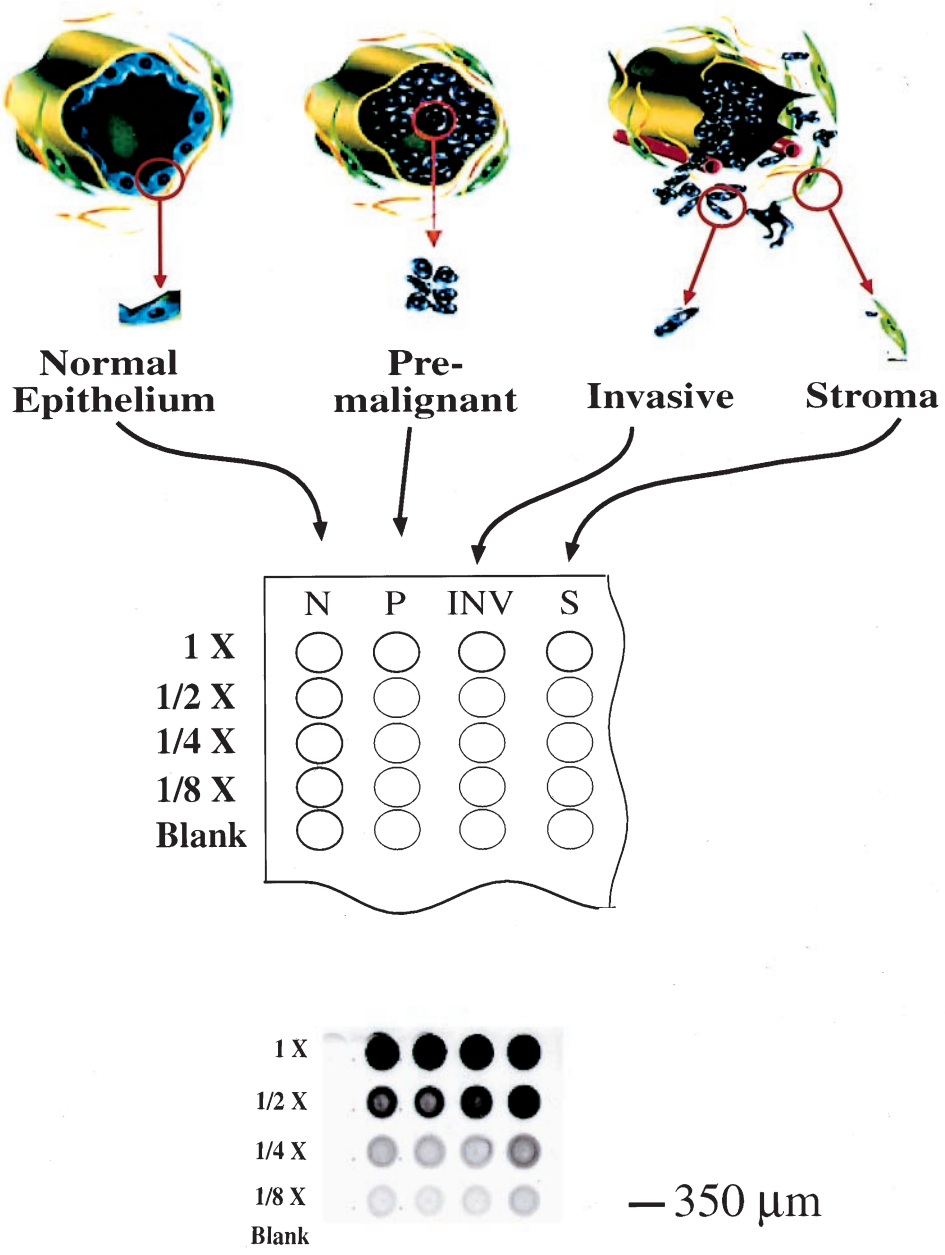

Figure 1 Schematic overview of longitudinal cancer progression investigation by cell captured lysate arraying. Defined patient matched cell populations are microdissected, lysed, and immobilized onto nitrocellulose slides at distinct positions. Each patient set is designed so that it contains its longitudinal cancer progression vertically, and corresponding dilution curves to each disease state horizontally. After arraying these slides are incubated with an antibody that can be detected by chemiluminescencent, florescencent, or colorimetric assays. Intensity of the signal is proportional to the concentration of the target protein

2000). A prospective study showed that the histologic progression of clinically detectable precursor lesions to esophageal cancer, i.e., mild, moderate and severe dysplasia, is associated with an increased invasive risk of developing invasive disease. To validate whether annexin-1 might serve as an early diagnostic marker we arrayed 10 different patient matched normal (N), low (L) and high grade (H) dysplasia, and invasive esophageal carcinoma (T) cell populations on one array from fully embedded esophageal resections. Slides in Figure 4a were probed against: (a) annexin-1 and to normalize protein loading; (b) actin. When identical arrayed slides were incubated with normal rabbit serum or secondary antibody alone no interaction was detected (data not shown). The adjusted expression protein level for each foci ($n=40$) was determined by dividing the median level of annexin-1 expression by the median level of actin expression. The mean adjusted annexin-1 expression for each histologic category decreased with increasing disease severity (N mean (standard error SE) 0.995 units (0.055), LG 0.707 (0.080), HG 0.611 (0.080), and CA 0.565 (0.045))

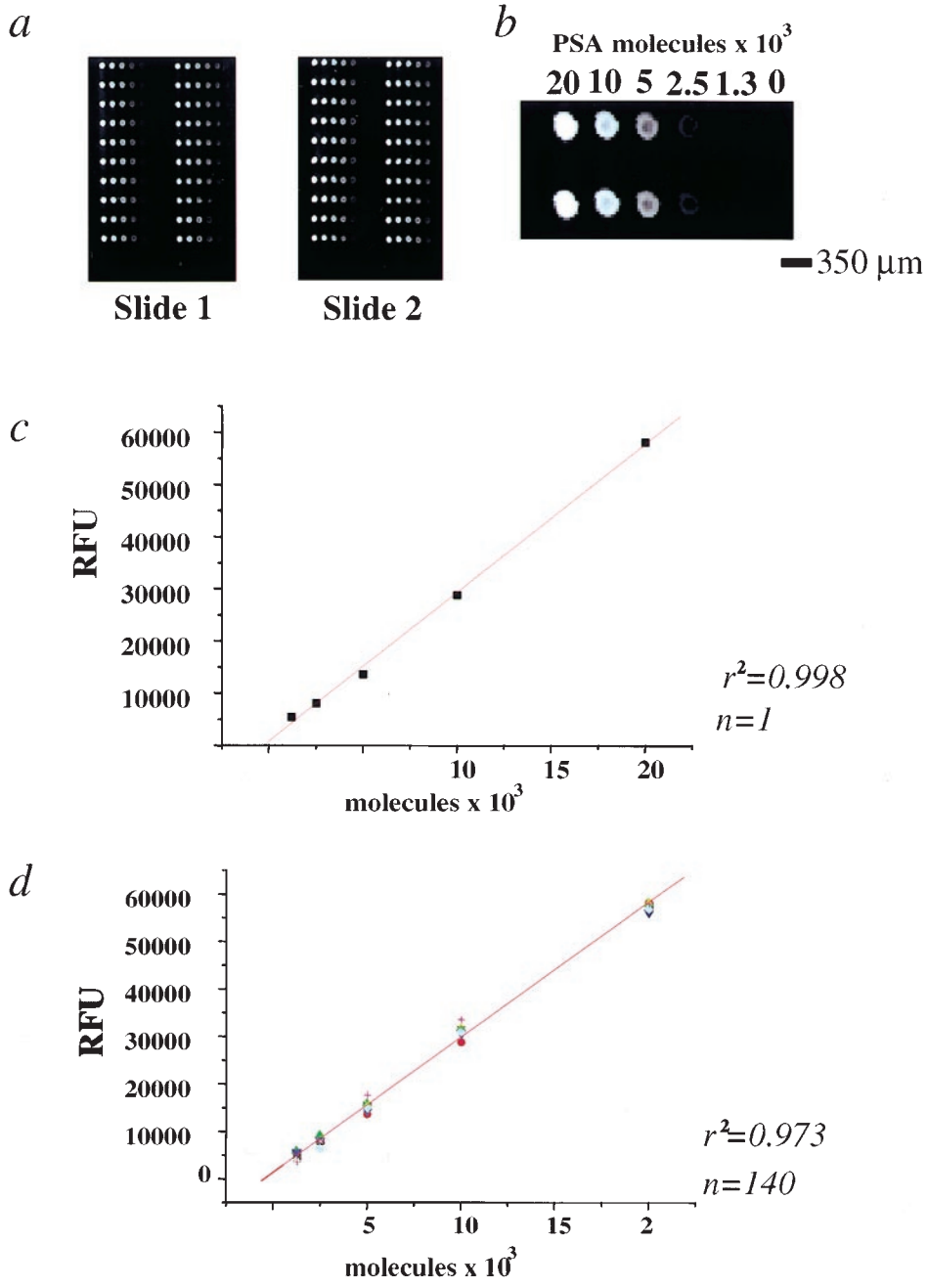

Figure 2 Precision and quantification validation of protein microarray. (**a**) Representative examples of two chromogen stained slides probed against PSA (n_{total} = 7). 20 dilution curves ranging from 20 000 to 1250 molecules of recombinant PSA were arrayed per slide. (**b**) Enlargement of ***a***. Average diameter of spot = 350 μm, average distance between spots = 800 μm. (**c**) Representative correlation between signal intensity and protein concentration of one dilution curve (correlation for all dilution curves ranged between $r^2 = 0.999$ and $r^2 = 0.990$). (**d**) Correlation for inter and intraspot linearity for the whole data set ($r^2 = 0.973$; $n = 140$)

(Figure 4b). Each disease category had significantly less protein expression of annexin-1 than normal epithelium ($P < 0.02$) for all comparisons. Specificity of antibodies was confirmed by Western blot analyses from the same cases (Figure 4c). These finding indicate: (a) that the reduction of annexin-1 protein is an early event in the pathogenesis of squamous esophageal cancer and appears to progressively decrease as the risk of developing invasive cancer increases; and (b) that the reverse phase array is a viable approach to the analysis of multiplexed proteomic outcomes.

Pro-survival and cell proliferation stimuli in prostate cancer progression.

It has been suspected that the Akt regulated pro-survival pathway and the mitogen kinase activated cell proliferation pathway may be disregulated during progression

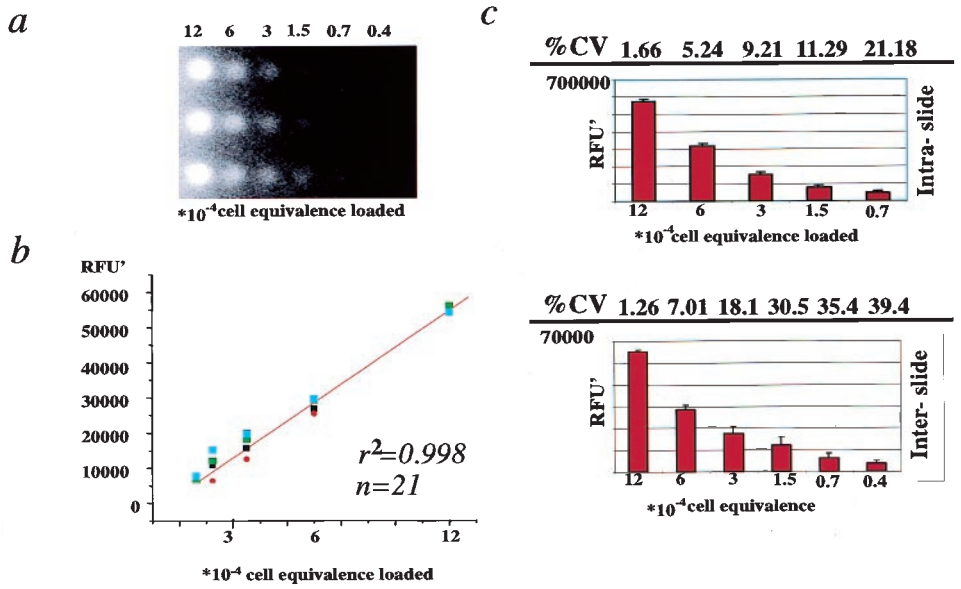

Figure 3 Validation of protein microarray for microdissected lysates. (**a**) Annexin-1 stained slide of triplicate arrayed dilution curves ranging from 120×10^{-4} to 4×10^{-4} cell equivalencies of microdissected normal esophageal epithelium. Experiment was carried out between seven arrayed slides yielding 21 datapoints per analysis per concentration. (**b**) Linear correlation between immobilized microdissected protein lysate and signal intensity between all seven slides ($r^2 = 0.953$). (**c**) Coefficient of variance for inter and intra spot reproducibility for all seven slides ranges from 1.66 and 1.25% to 21.18 and 39.4% (intra and inter spot, respectively) at the limit of detection indicating that the micro-application of cellular lysates procured by LCM can be achieved reproducibly

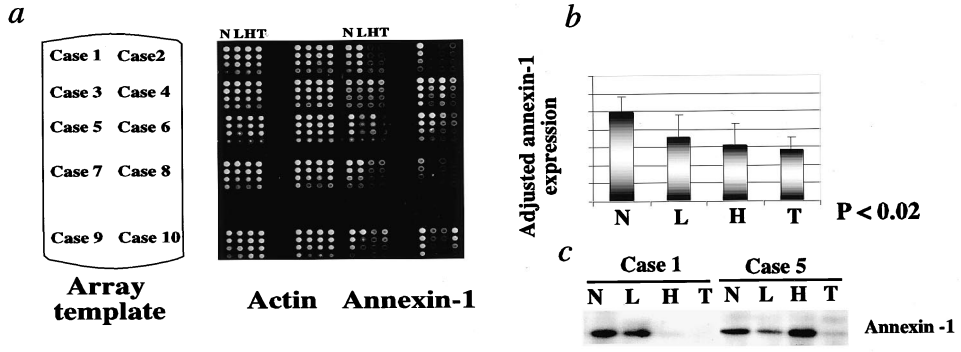

Figure 4 Disease associated candidate validation in human tissue. (**a**) Two identically arrayed slides probed against annexin-1 and actin. The slides were arrayed according to the template. Ten disparate cases containing patient matched normal (N), low (L) and high grade (H) dysplasia, and invasive esophageal carcinoma (T) from fully embedded esophageal resection were arrayed vertically with corresponding dilution curves horizontally. Detection of antibody was carried out in triplicates with one example shown here. (**b**) Statistically evaluation of adjusted annexin-1 expression by protein microarray: Each disease category had significantly less protein expression of annexin-1 (adjusted for actin protein expression) than normal epithelium (Wilcoxon rank-sum test for all comparisons $P < 0.012$. (**c**) Western blot analysis from the same cases probed against annexin-1 showed specificity and equal results than obtained by protein microarray

from normal to invasive cancer (Graff *et al*., 2000; Zimmermann and Moelling, 1999; Dimmeler and Zeiher, 2000; Franke *et al*., 1997; York *et al*., 1998). However this has not been previously studied in the context of longitudinal (i.e. patient matched normal, PIN, and invasive carcinoma) progression in the most biological relevant human tissue study sets. We analysed phosphorylated ERK, phosphorylated Akt, and cleaved PARP and Caspase 7 protein levels in patient matched normal (N), PIN (P), invasive carcinoma (T), and stroma (S) cell populations (Figure 5a–c). We found that in 10 out of 10 longitudinal cases phosphorylated ERK protein levels (normalized to total ERK) are suppressed during the evolution of progression ($P < 0.01$) with normal epithelium expressing highest level of phosphorylated ERK followed by a gradual decline with disease progression (Figure 5e). Total ERK levels were ubiquitously expressed with no detectable change in protein status per disease progression across all cases. Phosphorylated Akt levels concomitantly increased ($P < 0.03$) between normal and PIN, and between normal and invasive cancer ($P < 0.04$) (Figure 5e).

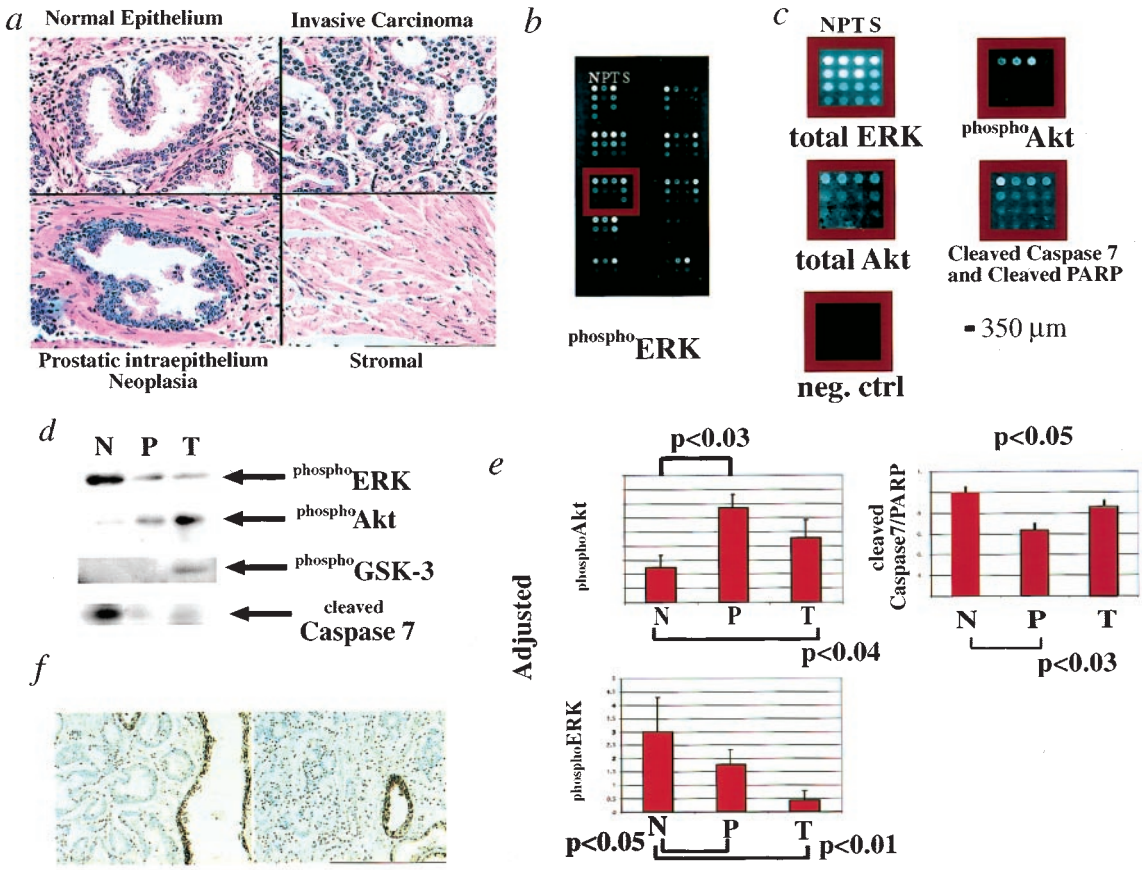

Figure 5 Pro-survival protein status in prostate cancer progression. (**a**) Representative H&E stained sections for histologically normal epithelium, prostatic intraepithelium neoplasia (PIN), invasive carcinoma, and stroma cell populations. (**b**) ^{phospho}ERK stained protein array of ten patient matched prostate progression cases. Array layout was as presented in Figure 1 with longitudinally disease progression arrayed vertically and corresponding dilution curves arrayed horizontally; N = histologically normal, P = PIN, T = invasive carcinoma, S = stroma. (**c**) Protein staining of total ERK, ^{phospho}Akt, total Akt, and cleaved caspase 7 and PARP protein levels for one case from protein array shown in **b**. All detectable signals were above signals obtained by negative control runs. (**d**) Specificity and validation of antibodies used by Western blot. Comparisons between the protein array arrays and Western blot analysis of nodal proteins involved in the pro-survival pathway yielded similar results. Western analyses on the apoptosis pathway directly affected by activated Akt showed suppression of downstream apoptosis pathways by phosphorylated GSK3-β (**e**) Statistically analysis for adjusted ^{phospho}ERK, ^{phospho}Akt, and cleaved Caspase 7 and cleaved PARP levels. Cancer progression was associated with increased phosphorylation of Akt ($P<0.03$ and $P<0.04$ for neoplastic transition from N to P and N to T, respectively), suppression of apoptosis pathways ($P<0.03$ and $P<0.05$, N to P and N to T, respectively), as well as decreased phosphorylation of ERK ($P<0.01$ for all comparisons). All statistical comparisons were carried out using the Wilcoxon rank-sum test. (**f**) Immunohistochemistry staining for two cases for ^{phospho}ERK confirming result obtained by Western blot analysis and reverse phase microarray

Subsequent study on cleaved PARP and cleaved Caspase 7 for these cases showed a direct relationship with increased activated Akt levels and decreased apoptosis between normal epithelium and PIN ($P<0.03$), and between normal and tumor ($P<0.05$). The highest change between activated Akt and subsequently cleaved Caspase 7 and PARP were observed between the neoplastic transition of normal to PIN. Specificity of these results was validated by micro Western analyses from microdissected relevant cell populations from the same cases for each antibody (Figure 5d). Subsequent studies by Western analyses from the same cases on the apoptosis pathway directly affected by Akt showed suppression of downstream apoptosis pathways through phosphorylation of glycogen syntase kinase-3 (GSK3-β) and cleaved caspase 7 (Figure 5d).

Discussion

Histopathologically, PIN represents the closest precursor lesion of prostatic tumorigenesis (Botswick, 1995). High grade PIN is characterized by specific nuclear and morphologic features, such as enlargement of nuclei and partial breakage of the basal membrane. Koch *et al*. and others have proposed that regulation of apoptosis and proliferation could lead to cell accumulation in PIN (Koch *et al*., 2000; Xie *et al*., 2000; Krajewaska *et al*., 1996). However, previous studies were based on immunohistochemistry and TUNEL assays applied to rat and human prostate tissue.

In the present study we now provide direct quantitative evidence that suppression of apoptosis in

PIN and invasive prostate cancer may be associated with phosphorylation of Akt and subsequent inactivation of its substrate GSK3-β. Akt has been shown to phosphorylate and inactivate GSK3-β/α both *in vitro* and *in vivo* (Cross *et al*., 1995). Subsequent studies on GSK3-β demonstrated that transfection of constitutively activated GSK3-β in Rat1 and PC 12 cell lines induces apoptosis, while overexpression of dominant negative mutant GSK3-β blocks apoptosis (Pap and Cooper, 1998). This suggests that cell survival through GSK-3 activity can be regulated by growth factors through the phosphatidyl-inositol 3-kinase-Akt pathway. Moreover we verify that downstream components of the apoptotic cascade (cleaved and non cleaved 7, as well as cleaved and non cleaved PARP) are also shifted toward pro-survival. This data is in keeping with known pro-survival pathways, which emanate from Akt through its substrates (Pap and Cooper, 1998; Yao and Cooper, 1995).

These results demonstrate a highly significant reduction in the ratio of phosphorylated ERK to total ERK during the longitudinal progression of human prostate cancer. High grade PIN exhibited a lower level of phospho-ERK compared to normal appearing epithelium. Invading carcinoma cells (average Gleason grade 6.6) contained phospho-ERK levels that were even further reduced compared to PIN. We confirmed this quantitative difference in phosphorylated ERK using immunohistochemistry on the same cases. Gioeli *et al*. (1999) conducted an immunohistochemistry study of prostate tumor tissue and reported low staining of phospho-ERK in tumors with a Gleason score of less than 7. The loss of sustained phospho-ERK during progression is in keeping with the antiproliferative effects of sustained ERK activity in cultured cells (Marshall, 1995; York *et al*., 1998; Frey and Mulder, 1997). Thus, during the transition to invasive carcinoma, suppression of sustained phosphorylation of ERK, known to cause a cell cycle block, may enable cellular proliferation.

These findings support a general hypothetical model of prostate cancer progression. Augmentation of the ratio of phosphorylated Akt to total Akt will suppress downstream apoptosis pathways through intermediate substrates such as GSK3-β. Reduction in apoptosis will shift the balance of cell birth and death rates favoring accumulation of cells within the prostate gland. Piling up of cells within the gland is a major pathologic hallmark of PIN. Pro-survival is required for migrating cells to resist the pro-apoptotic signals which take place during the disruption of integrin mediated adhesion to extracellular matrix molecules. In parallel, transient ERK activation, and augmentation of pro-survival pathways may be associated with cellular migration. Activation of Akt, a substrate of P13K, can therefore promote cell motility and survival as the invading cancer cells leave the gland and invade the stroma.

In conclusion, a novel protein array technology was developed and applied to gain previously unknown insights about specific molecular events taking place in microscopic disease progression within individual patients. This technology is broadly applicable to high-throughput molecular analysis of proteomic changes in tissue cells during development or disease, or after treatment. Genomic and proteomic initiatives are yielding growing catalogs of molecules which may be disease related, and thereby constitute candidates for diagnostic or therapeutic targets: (a) Is the candidate molecule actually present or altered in the human disease lesion?; (b) Does this alteration transcend patient anecdote to a molecular phenotype altered in a majority of patients; and (c) Is the candidate protein within a relevant pathway that can be verified to be aberrant in the diseased tissue chosen for treatment? The use of reverse phase microarrays may specifically target these questions.

Materials and methods

Materials

Fully embedded esophageal specimens ($n=40$) were obtained from patients who presented to the Shanxi Cancer Hospital in Taiyuan, People's Republic of China. These foci were longitudinally arrayed into ten cases comprising of normal, low and high-grade dysplasia, as well as invasive carcinoma from the same patient. Fourfold dilution curves of the each lysate were arrayed directly underneath each sample to ensure proper dynamic ranges for all antibodies tested. The Institutional Review Board (IRB) of the Shanxi Cancer Hospital and the US National Cancer Institute approved this study. Radical prostatectomy samples ($n=40$) were from men that presented with localized prostate cancer. Whole mounted sections were used for immunoblotting, immunohistochemistry and microdissection. Longitudinally matched foci were arrayed into 10 cases comprising of histologically normal epithelium, PIN, invasive cancer, and corresponding stroma cell population. Samples were fixed in 70% ethanol and completely embedded in paraffin. All specimens were studied anony-mously under a NIH IRB Waiver.

Microdissection and cellular lysate arraying

Microdissection was carried out under careful direct pathological examination as previously described using a Pixcell 200 Laser Capture Microdissection system (Arcturus Engineering, Mountain View, CA, USA). Briefly, prior to microdissection paraffin embedded tissue sections were deparaffinized by completely submersing the slide in Xylene three times for 6 min each and furthermore stained with a modified H&E staining protocol. The staining protocol calls for treatment of tissue sections sequentially in 100, 95, 70% ethanol, HPLC grade water, hematoxylin (Sigma, St. Louis, MO, USA), HPLC grade water, blueing solution (Sigma, St. Louis, MO, USA), 70, 95, 100% ethanol for 20 s each and final dehydration in Xylene. All staining baths contain 10 mmol Complete™ (Boehringer Mannheim, Germany) protease inhibitors. Between 500 and 3000 LCM shots (approximately 2500 and 15 000 cells, respectively) were acquired per investigated foci. For phosphorylated signaling molecules 3000 LCM pulses are the absolute minimum that needs to be microdissected. Microdissected cells were lysed in 30 μl of lysing buffer containing 1 : 1 mixture of 2 × SDS electrophoresis buffer (125 mM Tris pH 6.8, 4% SDS, 10% glycerol, 2% β-mercaptoethanol) and Tissue Protein Extraction Reagent (TPER, Pierce, Rockford, IL, USA) for 2 h at

70°C. After cell lysis samples were boiled beween 3 and 5 min each and 3 nl of the lysate were arrayed with a pin and ring GMSE 470 microarrayer (Affymetrix) using a 375 micron pin onto nitrocellulose slides with a glass backing (Schleicher and Schuell, Keene, NH, USA). Spatial densities of 980 spots/slide and greater can easily be accommodated on a 20 × 30 mm slide.

Staining was carried out on an automated slide stainer (Dako, Carpinteria, CA, USA) using the catalysed signal amplification system per manufacturer's recommendation (Dako, Carpinteria, CA, USA). Briefly, after micro application of cellular lysates the slides were treated for 15 min with Reblot™ (Chemicon, Temecula, CA, USA) and subsequently washed three times for 10 min each with TBS washing buffer (300 mmol NaC1, 0.1% Tween 20, 50 mmol Tris, pH 7.6). After treatment the arrays were blocked in a 0.5% casein solution for 30 min under constant rocking. Between each following step arrayed slides were washed three times 5 min each with TBS washing buffer. Endogenous biotin was blocked using the biotin blocking kit (Dako, Carpinteria, CA, USA) for 5 min, followed by application of protein block (Dako, Carpinteria, CA, USA) for 5 min, primary antibody diluted in antibody diluent (Dako, Carpinteria, CA, USA) at a concentration of 1 : 1000 for 30 min and finally secondary link antibody (Dako, Carpinteria, CA, USA) at a concentration of 1 : 100 for anti-mouse (diluted in antibody diluent) and neat for anti-rabbit for 30 min.

Amplification and staining was carried out as follows: The subsequent labeled microarray was treated with a streptaviding-biotin complex (Dako, Carpinteria, CA, USA) solution for 15 min, amplification reagent (biotinyl tyramide and hydrogen peroxidase) for 15 min, streptaviding-peroxidase for 15 min, and finally stained using 3,3′-diaminobenzidine tetrahydrochloride as chromogen. Excessive studies using a variety of staining methods (including chemiluminescent detection) showed this method to be superior with regard of sensitivity and signal to noise ratio. If chemiluminescent detection readout is desired arrayed nitrocellulose slides can be treated according to the protocol described for micro immunoblotting.

Specificity of each antibody was tested by Western blot. Antibodies were used at following concentrations: Rabbit anti-annexin-1 1 : 2500 (Zymed Laboratories, San Francisco, CA, USA), mouse anti-actin 1 : 4000 (Calbiochem, San Diego, CA, USA), mouse anti-PSA 1 : 4000 (Scripps Laboratories, San Diego, CA, USA), rabbit anti-Akt 1 : 500 (Cell Signaling, Beverly, MA, USA), rabbit anti-phosphoAkt 1 : 500 (Cell Signaling, Beverly, MA, USA), mouse anti-ERK 1 : 1000 (Transduction Laboratories, San Diego, CA, USA), rabbit anti-phosphoERK1/21 : 1000 (Cell Signaling, Beverly, MA, USA), rabbit anti cleaved-PARP and anti cleaved-caspase 7 1 : 500 (Cell Signaling, Beverly, MA, USA). Negative controls were carried out at following concentrations: isotype matched IgG mouse 1 : 1000 (Sigma, St. Louis, MO, USA), anti-mouse 1 : 100 (Dako, Carpinteria, CA, USA), anti rabbit neat (Dako, Carpinteria, CA, USA). Anti-phospho ERK (Cell Signaling, Beverly, MA, USA) recognizes phosphorylated threonine 202 and tyrosine 204 of p44 and p42. Specificity was confirmed by Western blot analysis.

Image and statistics analyses

Stained slides were scanned on a UMAX scanner with Adobe PhotoShop 5.5 at a resolution of 600 dpi for analyses. Scanned images (saved as tif. file) were analysed with Image Quant (Molecular Dynamics, Sunnyvale, CA, USA) using the 'histogram' option as background correction of choice. The Wilcoxon rank-sum test was used to test group differences in the adjusted mean protein expression between histologically normal epithelium, PIN, stroma, and invasive lesions. Two sided statistical tests are used throughout; P-values < 0.05 were considered to be statistically significant. All analyses were performed using the statistical software package STATA (STATA Corporation, College Station, TX, USA). Linear regression analysis and graphing were performed by Origin 4.1.

Immunoblotting

All antibodies were used at a concentration of 1 : 1000. Rabbit anti-annexin-1 (Zymed Laboratories, San Francisco, CA, USA), mouse anti-actin (Calbiochem, San Diego, CA, USA), (Scripps Laboratories, San Diego, CA, USA), rabbit anti-Akt (Cell Signaling, Beverly, MA, USA), rabbit anti-phosphoAkt (Cell Signaling, Beverly, MA, USA), mouse anti ERK (Transduction Laboratories, San Diego, CA, USA), rabbit anti-phosphoERK (Cell Signaling, Beverly, MA, USA), rabbit anti cleaved-PARP and anti cleaved-caspase 7 (Cell Signaling, Beverly, MA, USA), GSK3-β (Cell Signaling, Beverly, MA, USA), anti caspase 7 and anti PARP (Cell Signaling, Beverly, MA, USA). Western blotting was performed for 2 h using a BioRad SemiDry apparatus with Immobilon-P PVDF membrane (Millipore, Bedford, MA, USA) at a constant voltage of 25 V and 10A/10 cm^2. Chemiluminescent detection was carried out using CDP Star™ (Tropix, Bedford, MA, USA) per recommendations of the manufacture. Briefly, membranes were blocked in I-block supplemented with 0.01% v/v Tween 20 for 45 min and incubated with a primary antibody diluted in blocking buffer at a concentration of 1 : 1000 for 2 h. Membranes were washed three times for 5 min with blocking buffer after which the corresponding secondary antibody (1 : 5000) was incubated for 30 min. The blot was subsequently washed three times for 5 min with blocking buffer, rinsed twice with 1 × assay buffer and developed with CDP Star substrate supplemented with 1 : 20 dilution of Nitro Block II until bands were clearly visible.

Acknowledgments

We thank Dr Phil R Taylor of the Cancer Prevention Studies Branch, National Cancer Institute, Bethesda, Maryland, USA, and Drs Quan-Hong Wang, Wen-Jie Guo and Yong-Zhen Zhang of the Shanxi Cancer Hospital and Institute, Taiyuan, Shanxi, China for coordinating and conducting all the field related and tissue procurement activities in China.

References

Arenkov P, Kukhtin A, Gemmell A, Voloshchuk S, Chupeeva V and Mirzabekov A. (2000). *Anal. Biochem.,* **278,** 123 – 131.

Bostwick DG. (1995). *Cancer,* **75,** 1823 – 1836.

Buckholtz RG, Simmons CA, Stuart JM and Weiner MP. (1999). *J. Mol. Microbiol. Biotechnol.,* **1,** 135 – 140.

Cross DAE, Alessi DR, Cohen P, Adndjelkovich M and Hedmmings BA. (1995). *Nature,* **378,** 785 – 788.

DeRisi J, Penland L, Brown PO, Bittner ML, Meltzer PS, Ray M, Chen Y, Su YA and Trent JM. (1996). *Nat. Genet.,* **4,** 457 – 460.
Dimmeler S and Zeiher AM. (2000). *Circ. Res.,* **86,** 4 – 5.
Ekins RP and Chu FW. (1991). *Clin. Chem.,* **37,** 1955 – 1967.
Emili AQ and Cagney G. (2000). *Nat. Biotechnol.,* **18,** 393 – 397.
Emmert-Buck MR, Bonner RF, Smith PD, Chuaqui RF, Zhuang Z, Goldstein S and Liotta LA. (1996). *Science,* **274,** 1481 – 1483.
Emmert-Buck MR, Gillespie JW, Paweletz CP, Ornstein DK, Basrur V, Appella E, Wang QH, Huang J, Hu N, Taylor P and Petricoin III EF. (2000). *Mol. Carcinog.,* **27,** 158 – 165.
Englert CR, Baibakov GV and Emmert-Buck MR. (1999). *Cancer Res.,* **60,** 1526 – 1530.
Fodor SPA, Read JL, Pirrung MC, Stryer L, Lu AT and Solas D. (1991). *Science,* **251,** 767 – 773.
Franke TF, Kaplan DR and Cantley LC. (1997). *Cell,* **88,** 435 – 437.
Frey RS and Mulder KM. (1997). *Cancer Res.,* **57,** 628 – 633.
Ge H. (2000). *Nucleic Acid Res.,* **28,** e3.
Gioeli D, Mandell JW, Petroni GR, Frierson Jr HF and Weber MJ. (1999). *Cancer Res.,* **59,** 279 – 284.
Graff JR, Konicek BW, McNulty AM, Wang ZJ, Houck K, Allen S, Paul JD, Hbaiu A, Goode RG, Sandusky GE, Vessella RL and Neubauer BL. (2000). *JBC.,* **275,** 24500 – 24505.
Haab BB, Dunham JM and Brown PO. (2001). *Genome Biology,* **2,** 1 – 13.
Hanahan D and Weinberg RA. (2000). *Cell,* **100,** 57 – 70.
Jones WV, Kenseth JR, Porter MD, Mosher CL and Henderson E. (1998). *Anal. Chem.,* **70,** 1233 – 1241.
Koch M, Miguel M, de Hoefler H and Diaz-Cano SJ. (2000). *Virchows Arch.,* **436,** 413 – 420.
Kononen J, Bubendorf L, Kallioniemi A, Bärlund M, Schraml P, Leighton S, Torhorst J, Mihatsch MJ, Sauter G and Kallioniemi OP. (1998). *Nat. Med.,* **4,** 844 – 847.
Krajewaska M, Krajewski S, Epstein JI, Shabaik A, Sauvageot J, Song K, Kitada S and Reed JC. (1996). *Am. J. Pathol.,* **1148,** 1567 – 1576.
Lipshutz RJ, Fodor SP, Gingeras TR and Lockhart DJ. (1999). *Nat. Genet.,* **1** (suppl), 20 – 24.
Lueking A, Horn M, Eickhoff H, Büssow K, Lehrach H and Walter G. (1999). *Anal. Biochem.,* **270,** 103 – 111.
MacBeath G, Koehler AN and Schreiber SL. (1999). *JACS,* **121,** 7966 – 7968.
Marshall CJ. (1995). *Cell,* **80,** 179 – 185.
Ornstein DK, Gillespie JW, Paweletz CP, Duray PH, Herring J, Vocke CD, Topalian SZ, Bostwick DG, Linehan WM, Petricoin III EF and Emmert-Buck MR. (2000). *Electrophoresis,* **21,** 2235 – 2242.
Page MJ, Amess B, Townsend RR, Parekh R, Herath A, Brusten L, Zvelebil MJ, Stein RC, Waterfield MD, Davies SC and O'Hare MJ. (2000). *PNAS,* **96,** 12589 – 12594.
Pap M and Cooper GM. (1998). *JBC,* **273,** 19929 – 19932.
Paweletz CP, Ornstein DK, Roth MJ, Bichsel VE, Gillespie JW, Calvert VS, Vocke CD, Hewitt SM, Duray PH, Herring J, Wang QH, Hu N, Lineham WM, Taylor PR, Liotta LA, Emmert-Buck MR and Petricoin EF. (2000). *Cancer Res.,* **60,** 6293 – 6297.
Rowe AC, Tender LM, Feldstein MJ, Golden JP, Scruggs SB, MacCraith BD, Cras JJ and Ligler FS. (1999). *Anal. Chem.,* **71,** 3846 – 3852.
Schena M, Shalon D, Davis RW and Brown PO. (1995). *Science,* **270,** 467 – 470.
Williams KL and Hochstrasser DF. (1997). *Proteome Research: New Frontiers in Functional Genomics*. Wilkins MR, Williams KL, Appel RD and Hochstrasser DF (eds). Springer: Berlin, Germany, 1 – 11.
Xie W, Wong YC and Tsao SW. (2000). *Prostate,* **44,** 31 – 39.
Yao R and Cooper G. (1995). *Science,* **267,** 2003 – 2006.
York RD, Yao H, Dillon T, Ellig CL, Eckert SP, McClesky EW and Stork PJS. (1998). *Nature,* **392,** 622 – 626.
Zheng DQ, Woodward AS, Tallini G and Languino LR. (2000). *JBC,* **275,** 24565 – 24574.
Zimmermann S and Moelling K. (1999). *Science,* **286,** 1741 – 1744.